Virologica Sinica 40 (2025) 324–332

Contents lists available at ScienceDirect

Virologica Sinica

journal homepage: www.keaipublishing.com/en/journals/virologica-sinica
www.virosin.org

Research Article

The SARS-CoV-2 3CL protease inhibits pyroptosis through the cleavage of gasdermin D

Yecheng Zhang [a], Xinlei Ji [b], Dan Huang [b], Gen Lu [a,*], Xinwen Chen [b,*]

[a] Department of Respiratory, Guangzhou Women and Children's Medical Center, Guangzhou Medical University, Guangzhou, Guangdong 510623, China
[b] Guangzhou National Laboratory, Guangzhou 510005, China

ARTICLE INFO

Keywords:
SARS-CoV-2
3C-like (3CL) protease
Gasdermin D (GSDMD)
Pyroptosis

ABSTRACT

Severe acute respiratory syndrome coronavirus 2 (SARS-CoV-2), the causative agent of novel coronavirus disease 2019, can cause acute respiratory symptoms and even death globally. However, the immune escape mechanism and viral pathogenesis remain poorly understood. Here, we report that the SARS-CoV-2 3C-like (3CL) protease specifically cleaves gasdermin D (GSDMD) at Q29 and Q193, producing two N-terminal fragments, $GSDMD_{1–29}$ and $GSDMD_{1–193}$. We also found that SARS-CoV-2 infection induced the cleavage of GSDMD. Then, we demonstrated that the ability to cleave GSDMD was dependent on the protease activity of the 3CL protease. Interestingly, unlike the $GSDMD_{1–275}$ fragment cleaved by caspase-1, $GSDMD_{1–29}$ and $GSDMD_{1–193}$ did not trigger pyroptosis or inhibit SARS-CoV-2 replication. Additionally, various RNA viral proteases display different preferences for cleaving GSDMD at Q29 and Q193. Our findings reveal a mechanism by which SARS-CoV-2 and other RNA viruses inhibit pyroptosis, highlighting the critical role of the 3CL protease in immune evasion and viral replication.

INTRODUCTION

Novel coronavirus disease 2019 (COVID-19), caused by severe acute respiratory syndrome coronavirus 2 (SARS-CoV-2) infection, is an acute respiratory illness characterized by fever, cough, fatigue, and breathing difficulties (Zhou et al., 2020). In severe cases, it can lead to pneumonia, acute respiratory distress syndrome, renal failure, and death. Since its emergence in 2019, SARS-CoV-2 has become a global health threat.

SARS-CoV-2 belongs to the *β-coronavirus* family, similar to SARS-CoV and Middle East respiratory syndrome coronavirus (MERS-CoV) (Fung et al., 2021). The 5′ end of the SARS-CoV-2 genome encodes two polyproteins, polyprotein 1a (pp1a) and polyprotein 1 ab (pp1ab), which are primarily cleaved by the 3C-like protease (3CL protease, also known as Nsp5) into functional proteins essential for viral replication (Yang and Rao, 2021). The highly conserved 3CL protease sequence across coronaviruses makes it a promising target for broad-spectrum antivirals (Anand et al., 2003; Yang et al., 2005). The SARS-CoV-2 3CL protease is also widely involved in virus and host interactions, such as by cleaving RNF20 to promote viral replication (Zhang S. et al., 2021), increasing cytokine production and the inflammatory response by cleaving NLRP12 and TAB1 (Moustaqil et al., 2021), and inducing inflammasome activation by cleaving NLRP1 or CARD8 (Planès et al., 2022; Tsu et al., 2023).

Pyroptosis, a lytic form of programmed cell death, is characterized by cell swelling, the formation of pores on the cytoplasmic membrane, lysis and the release of cytoplasmic contents (Jorgensen and Miao, 2015; Broz and Dixit, 2016). The executioner protein gasdermin D (GSDMD) is cleaved by inflammatory caspases, and the resulting $GSDMD_{1–275}$ fragment forms pores in the cell membrane, triggering pyroptosis (Shi et al., 2015; Liu et al., 2016; Zheng et al., 2020). Pyroptosis eliminates infected cells and restricts viral spread during infection (Yogarajah et al., 2017; Zhu et al., 2017). SARS-CoV-2 directly activates GSDMD, which triggers NET production and organ damage in patients with COVID-19 (Silva et al., 2022). Various viruses, including SARS-CoV-2, modulate pyroptosis for immune evasion. For example, the proteases of enterovirus 71 (EV71) and porcine epidemic diarrhea virus (PEDV) inhibit pyroptosis by cleaving GSDMD at Q193 (Lei et al., 2017; Shi et al., 2022). Additionally, nucleocapsid of SARS-CoV-2 suppresses host pyroptosis by binding GSDMD and blocking its cleavage (Ma et al., 2021). Most recently, it was reported that the SARS-CoV-2 3CL protease inhibited pyroptosis by cleaving GSDMD at Q29 and Q193 (Shen et al., 2024).

* Corresponding authors.
E-mail addresses: chen_xinwen@gzlab.ac.cn (X. Chen), lugen5663330@sina.com (G. Lu).

https://doi.org/10.1016/j.virs.2025.03.006
Received 7 November 2024; Accepted 17 March 2025
Available online 19 March 2025

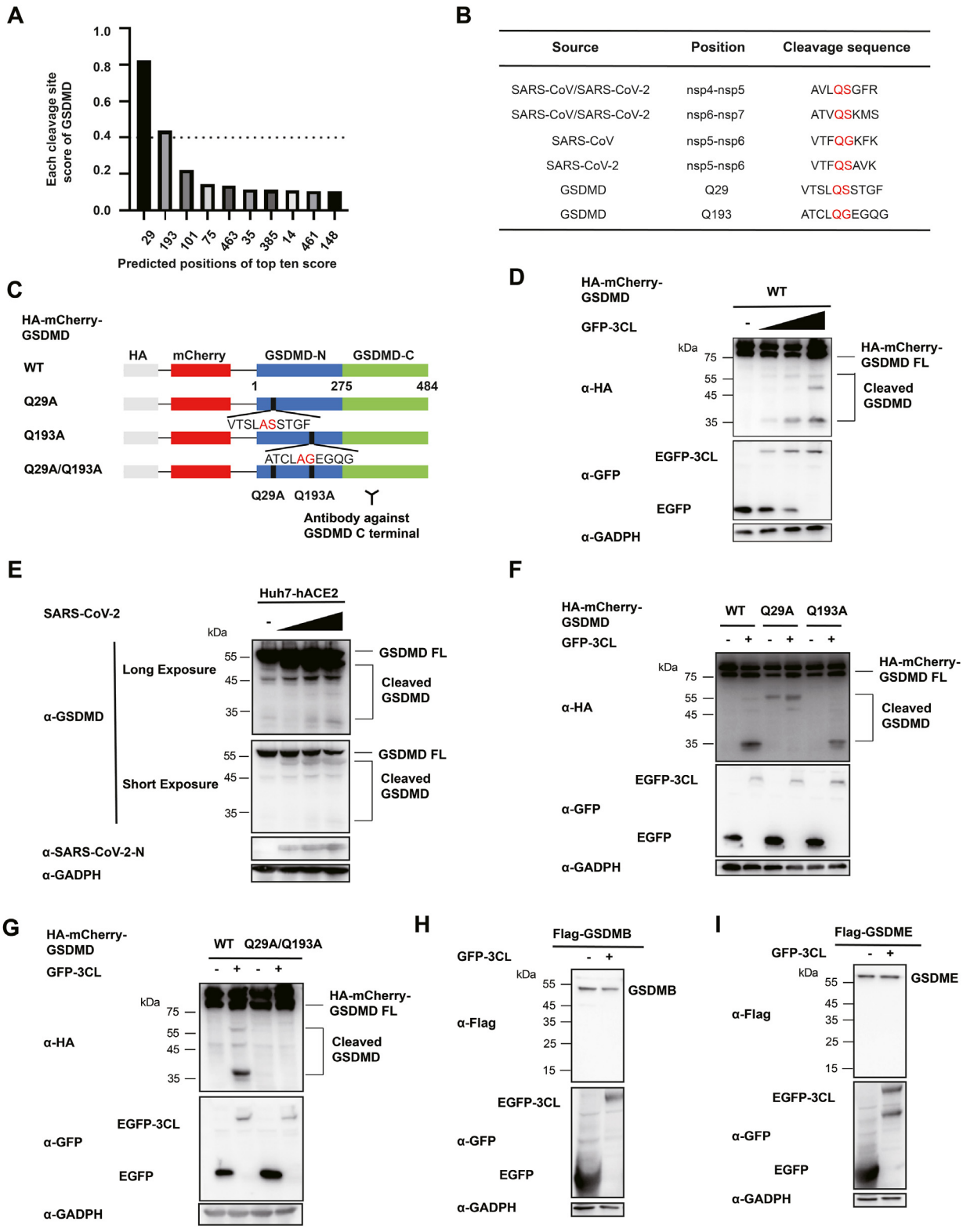

Fig. 1. The SARS-CoV-2 3CL protease cleaves GSDMD at Q29 and Q193. **A** The top ten GSDMD cleavage sites predicted by NetCorona. **B** Comparison of known 3CL protease cleavage sites in Nsp4, Nsp6, and Nsp5 with predicted sites in GSDMD, the cleavage sites recognized by 3CL protease on different proteins were labeled in red. **C** The schematic illustrates the mutations of GSDMD Q29A, Q193A, and Q29A/Q193A, where the QS and QG motifs on the GSDMD protein, as predicted by NetConora, have been mutated to AS and AG, respectively, and these mutated sites are highlighted in red. **D** Western blot analysis of GSDMD cleavage by increasing amounts of GFP-3CL in 293T cells. **E** Western blot analysis was conducted to assess the cleavage of GSDMD in Huh7-ACE2 cells infected with SARS-CoV-2 at various multiplicities of infection (MOIs) of 0.01, 0.1, and 1. The exposure times for the GSDMD protein are indicated as short exposure for 1 s and long exposure for 5 s in this image. **F** Western blot analysis of wild-type and single mutant (Q29A or Q193A) GSDMD cleavage by GFP-3CL. **G** Western blot analysis of wild-type and double mutant (Q29A/Q193A) GSDMD cleavage by GFP-3CL. **H** and **I** Western blot analysis of Flag tagged GSDMB (**H**) and GSDME (**I**) cleavage by GFP-3CL of SARS-CoV-2 in 293T cells.

It was predicted that the SARS-CoV-2 3CL protease may cleave GSDMD at both Q29 and Q193 using NetCorona. Here, we report that the SARS-CoV-2 3CL protease cleaves GSDMD to produce $GSDMD_{1–29}$ and $GSDMD_{1–193}$ at Q29 and Q193 during SARS-CoV-2 infection. Compared with $GSDMD_{1–275}$, these cleaved forms of GSDMD do not induce pyroptosis or inhibit viral replication. Furthermore, our study demonstrated that different viral proteases exhibit varying preferences for cleavage sites at Q29 and Q193. These findings elucidate the mechanism by which SARS-CoV-2 inhibits pyroptosis through the 3CL protease, underscoring the critical role of the 3CL protease in immune evasion and viral propagation.

RESULTS

The SARS-CoV-2 3CL protease cleaves GSDMD at Q29 and Q193

Using NetCorona, which predicts coronavirus 3CL protease cleavage sites, we identified Q29 and Q193 of GSDMD as potential cleavage sites, with scores of 0.826 and 0.438, respectively (Fig. 1A). These residues follow the Q-G/Q-S consensus sequence for the SARS-CoV-2 and SARS-CoV 3CL proteases (Fig. 1B). To detect GSDMD N-terminal fragments, we generated an HA-mCherry-GSDMD construct (Fig. 1C). In 293T cells cotransfected with GFP-tagged 3CL protease (GFP-3CL) and HA-mCherry-GSDMD, we observed two cleaved bands at approximately 55 kDa and 35 kDa, in addition to the full-length 80 kDa band, suggesting GSDMD cleavage at these two sites (Fig. 1D). These cleaved bands increased in a dose-dependent manner with increasing GFP-3CL expression (Fig. 1D).

In Huh7-ACE2 cells infected with SARS-CoV-2, we observed a dose-dependent decrease in full-length GSDMD (55 kDa) and a concomitant increase in two cleaved bands at approximately 50 kDa and 30 kDa (Fig. 1E). Mutational analysis using the Q29A, Q193A, and Q29A/Q193A mutants (Fig. 1C) confirmed that the 3CL protease cleaves GSDMD at both Q29 and Q193. While wild-type GSDMD produced two cleaved bands, the Q29A or Q193A mutants generated only one cleaved band, and cleavage of the Q29A/Q193A double mutant was abolished (Fig. 1F and G).

To investigate the specificity of the SARS-CoV-2 3CL protease in cleaving members of the gasdermin (GSDM) family, specifically GSDMB and GSDME, we cloned and co-transfected Flag-tagged GSDMB or GSDME with the SARS-CoV-2 3CL protease into 293T cells. Western blot analysis revealed that the 3CL protease did not cleave either GSDMB or

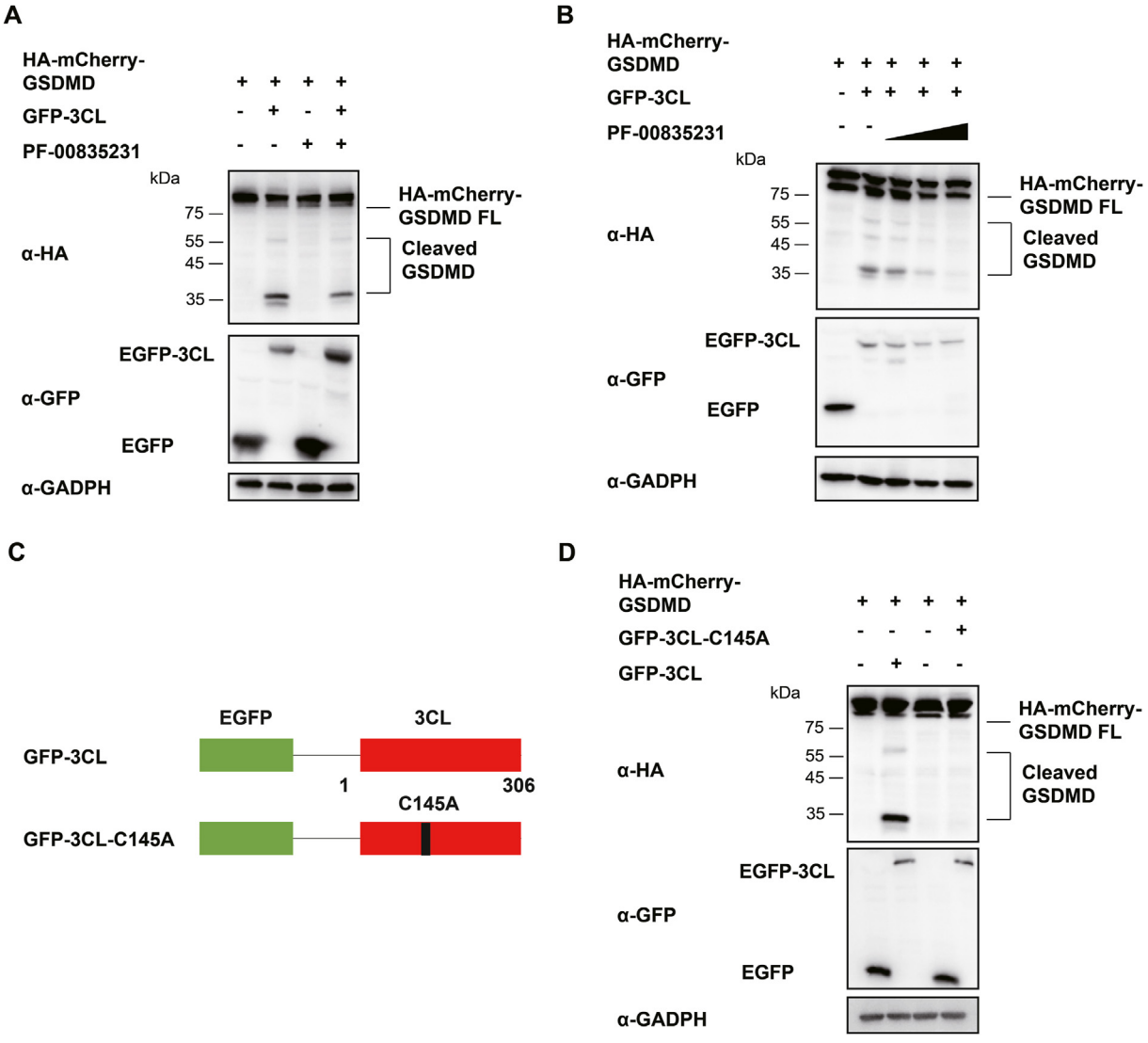

Fig. 2. 3CL protease activity is required for GSDMD cleavage. **A** Western blot analysis of GSDMD cleavage by GFP-3CL with or without 10 μM PF-00835231 treatment. **B** Dose-dependent inhibition of GSDMD cleavage by a series of 10-fold diluted PF-00835231 at concentrations of 1 μM, 10 μM and 100 μM. **C** Schematic of the 3CL protease C145A mutation. **D** Western blot analysis of GSDMD cleavage by the wild-type and C145A mutant 3CL proteases from SARS-CoV-2.

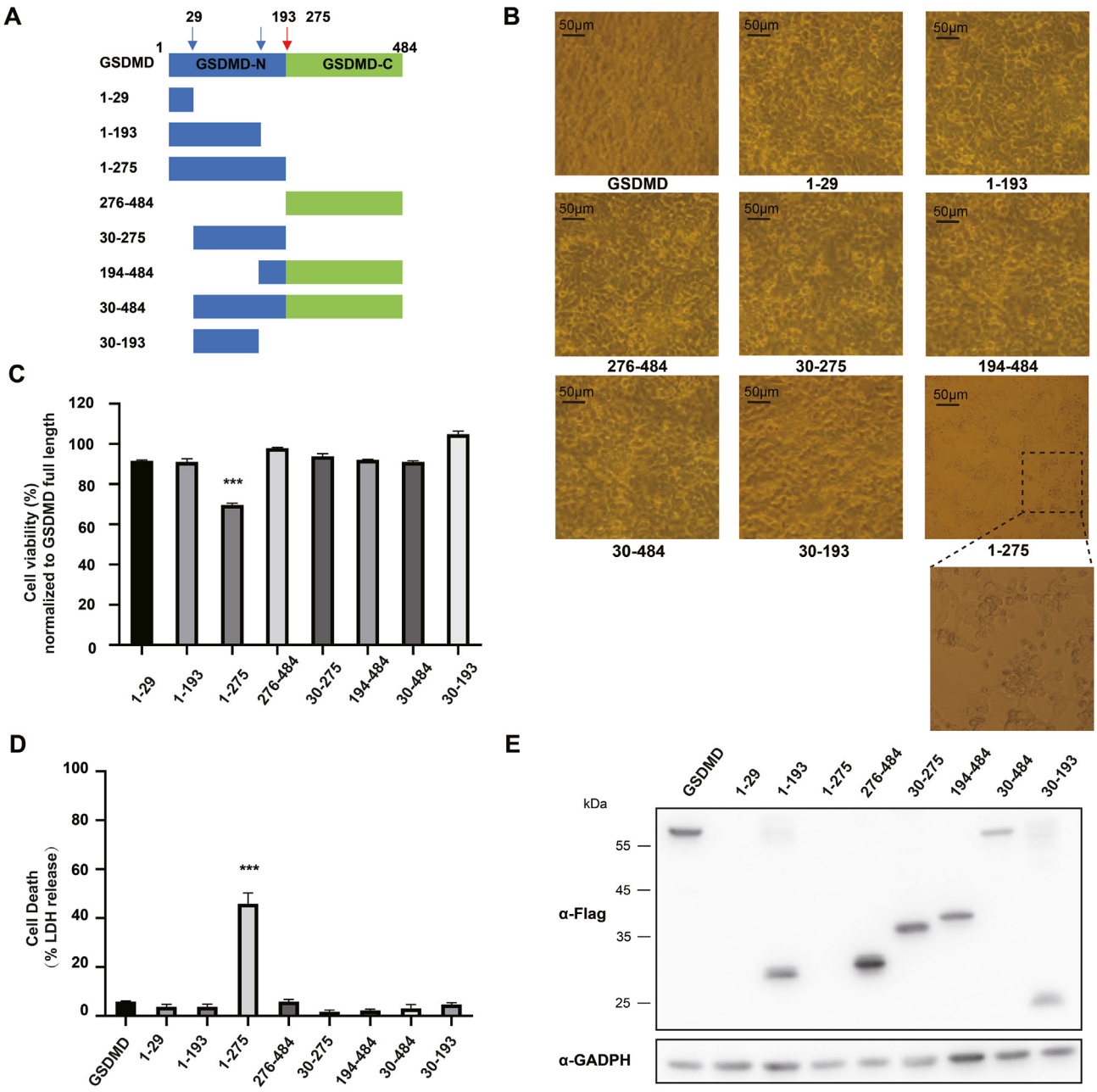

Fig. 3. 3CL protease-cleaved GSDMD fragments do not induce pyroptosis. **A** Schematic of GSDMD and its cleaved fragments. **B** Morphological changes in 293T cells expressing 3 × Flag-tagged GSDMD fragments. 293T cells were transfected with indicated plasmids, the morphological changes of cells were observed by optical microscope at 24 h after transfection. Viability (**C**) and LDH release (**D**) of 293T cells expressing 3 × Flag-tagged GSDMD fragments. 293T cells were treated as described in panel B, cell viability was assessed using the CCK-8 assay, and cell death was measured by LDH release using an LDH Release Assay Kit. **E** Western blot analysis of 3 × Flag-tagged GSDMD fragment expression. 293T cells were treated as described in panel B, cells were lysed and analyzed by Western blotting. Two-tailed Student's *t*-test was used for two-group comparisons. ***, $P < 0.001$.

GSDME proteins (Fig. 1H and I). These findings demonstrate that the SARS-CoV-2 3CL protease exhibits specificity for cleaving GSDMD and does not cleave other GSDM family members tested in this study.

Cleavage of GSDMD depends on 3CL protease activity

Treatment with the SARS-CoV-2 3CL protease inhibitor PF-00835231 blocked GSDMD cleavage in a dose-dependent manner (Fig. 2A and B), indicating that cleavage of GSDMD requires protease active of 3CL protease. Cys145 plays a crucial role in SARS-CoV-2 3CL protease activity (Jin et al., 2020; Zhang et al., 2020). The catalytically inactive C145A mutant of the 3CL protease failed to cleave GSDMD, despite exhibiting expression levels comparable to the wild type (Fig. 2C and D). These results demonstrate that GSDMD cleavage is dependent on the protease activity of the SARS-CoV-2 3CL protease.

Cleavage of GSDMD by the 3CL protease does not induce pyroptosis

GSDMD is cleaved by inflammatory caspases to generate $GSDMD_{1–275}$, which induces pyroptosis via the formation of plasma membrane pores (Sborgi et al., 2016; Shi et al., 2022). To investigate the

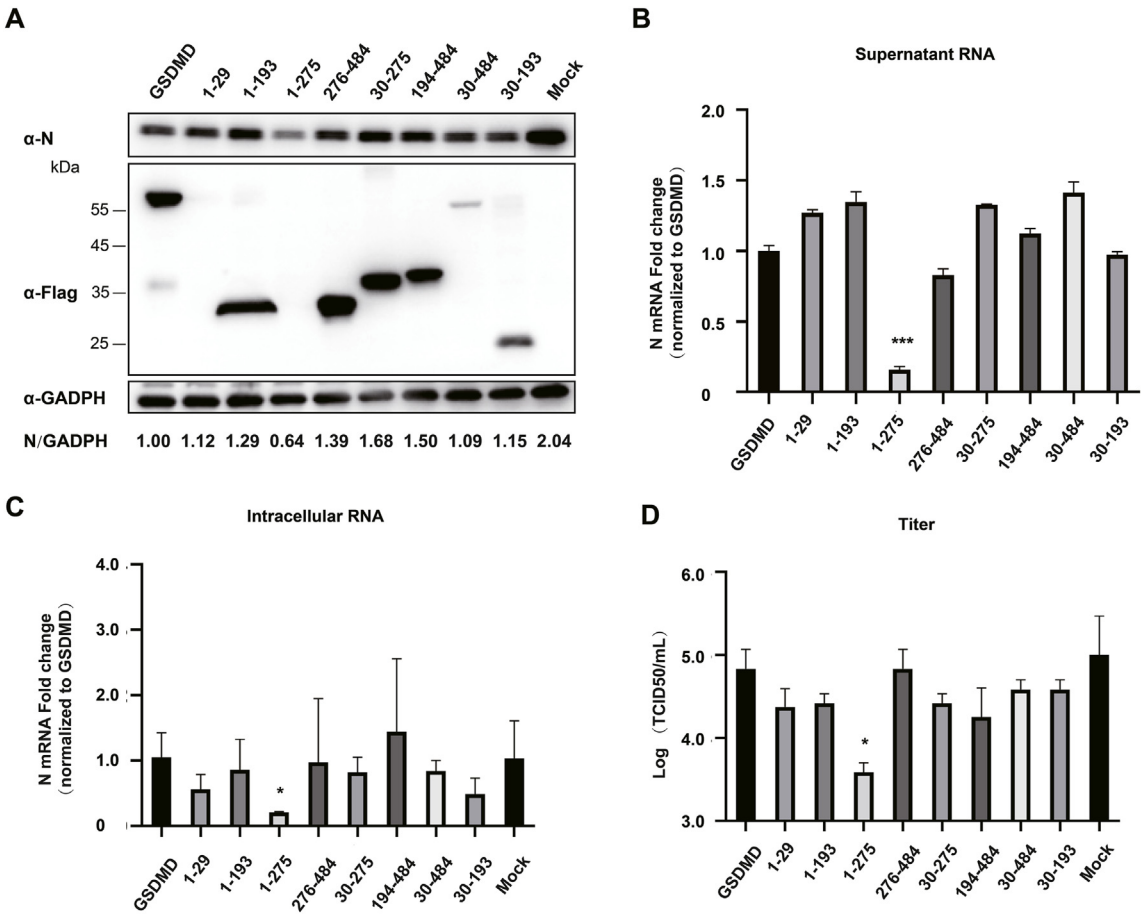

Fig. 4. 3CL protease-cleaved GSDMD fragments do not inhibit SARS-CoV-2 replication. **A** Western blot analysis of the SARS-CoV-2 N protein in H1299-ACE2 cells expressing GSDMD fragments. H1299-ACE2 cells were transfected with indicated plasmids. At 24 h after transfection, cells were infected with SARS-CoV-2 at an MOI of 0.01. After 24 h post infection, cells were lysed and analyzed by Western blotting. **B–C** qRT-PCR analysis of intracellular (**B**) and supernatant (**C**) SARS-CoV-2 RNA levels. H1299-ACE2 cells were treated as described in panel A, the intracellular and supernatant SARS-CoV-2 RNA levels were evaluated by quantitative real-time PCR. Data are expressed as fold change of the viral mRNA level, normalized to GSDMD. **D** $TCID_{50}$ assay of viral titres in supernatants. Two-tailed Student's *t*-test was used for two-group comparisons. *, $P < 0.05$; ***, $P < 0.001$.

effect of SARS-CoV-2 3CL protease-mediated GSDMD cleavage on pyroptosis, we constructed various 3 × Flag GSDMD truncations to mimic inflammatory caspases and 3CL protease cleavage products (Fig. 3A). In 293T cells, only $GSDMD_{1–275}$ induced pyroptosis, which was characterized by typical morphological features (Fig. 3B), decreased cell viability (Fig. 3C), and increased LDH release (Fig. 3D). Other GSDMD fragments, including those cleaved by the 3CL protease, did not induce pyroptosis (Fig. 3B and D). Protein expression was confirmed by western blotting, except for $GSDMD_{1–275}$ and $GSDMD_{1–29}$ (Fig. 3E). The inability to detect $GSDMD_{1–29}$ may be attributed to the extremely small size (approximately 3 kDa), whereas the undetectable expression of $GSDMD_{1–275}$ may be due to its potential to induce cell pyroptosis. Taken together, these results indicate that the fragments of GSDMD cleaved by the 3CL protease are unable to induce pyroptosis.

Effect of the cleaved GSDMD fragment on SARS-CoV-2 replication

Previous studies reported that several viral proteases can cleave GSDMD to affect pyroptosis, resulting in the regulation of viral replication (Lei et al., 2017; Zhao et al., 2022); therefore, we wanted to examine the impact of GSDMD cleavage products on SARS-CoV-2 replication in H1299-ACE2 cells, a cell line suitable for SARS-CoV-2 growth (Yao et al., 2023). $GSDMD_{1–275}$ significantly decreased viral N protein expression (Fig. 4A), supernatant and intracellular RNA levels (Fig. 4B and C), and infectious titres (Fig. 4D). Other GSDMD fragments, including $GSDMD_{1–29}$ and $GSDMD_{1–193}$ produced by 3CL protease cleavage, did not inhibit viral replication (Fig. 4A–D). These results suggest that the SARS-CoV-2 3CL protease cleaves GSDMD to generate $GSDMD_{1–29}$ and $GSDMD_{1–193}$, inhibiting $GSDMD_{1–275}$-mediated pyroptosis and promoting viral replication.

Different RNA viral proteases have varying preferences for GSDMD cleavage sites

Several viruses in the *Coronaviridae* and the *Picornaviridae* families have similar abilities to encode viral 3CL proteases (Tsu et al., 2021). We compared the cleavage effects of the 3CL proteases from SARS-CoV and MERS-CoV, as well as the 3C protease from EV71, on GSDMD. While the 3CL proteases of SARS-CoV and MERS-CoV cleaved HA tagged GSDMD (about 80 kDa) at both Q29 and Q193, producing two bands (55 kDa and 35 kDa) (Fig. 5A and B), the EV71 3C protease cleaved HA tagged GSDMD only at Q193, generating a single 55 kDa band (Fig. 5C). Mutational analysis using the Q29A, Q193A, and Q29A/Q193A mutants of GSDMD confirmed the cleavage site preferences mentioned above (Fig. 5A–C). These findings demonstrate that different RNA viral proteases have distinct preferences for cleaving GSDMD at Q29 and Q193. To further confirm whether the cleavage of GSDMD by SARS-CoV and MERS-CoV proteases is dependent on their proteolytic activity, we initially constructed enzyme activity mutants of the SARS-CoV and MERS-CoV 3CL proteases, designated as SARS-3CL-C145A and

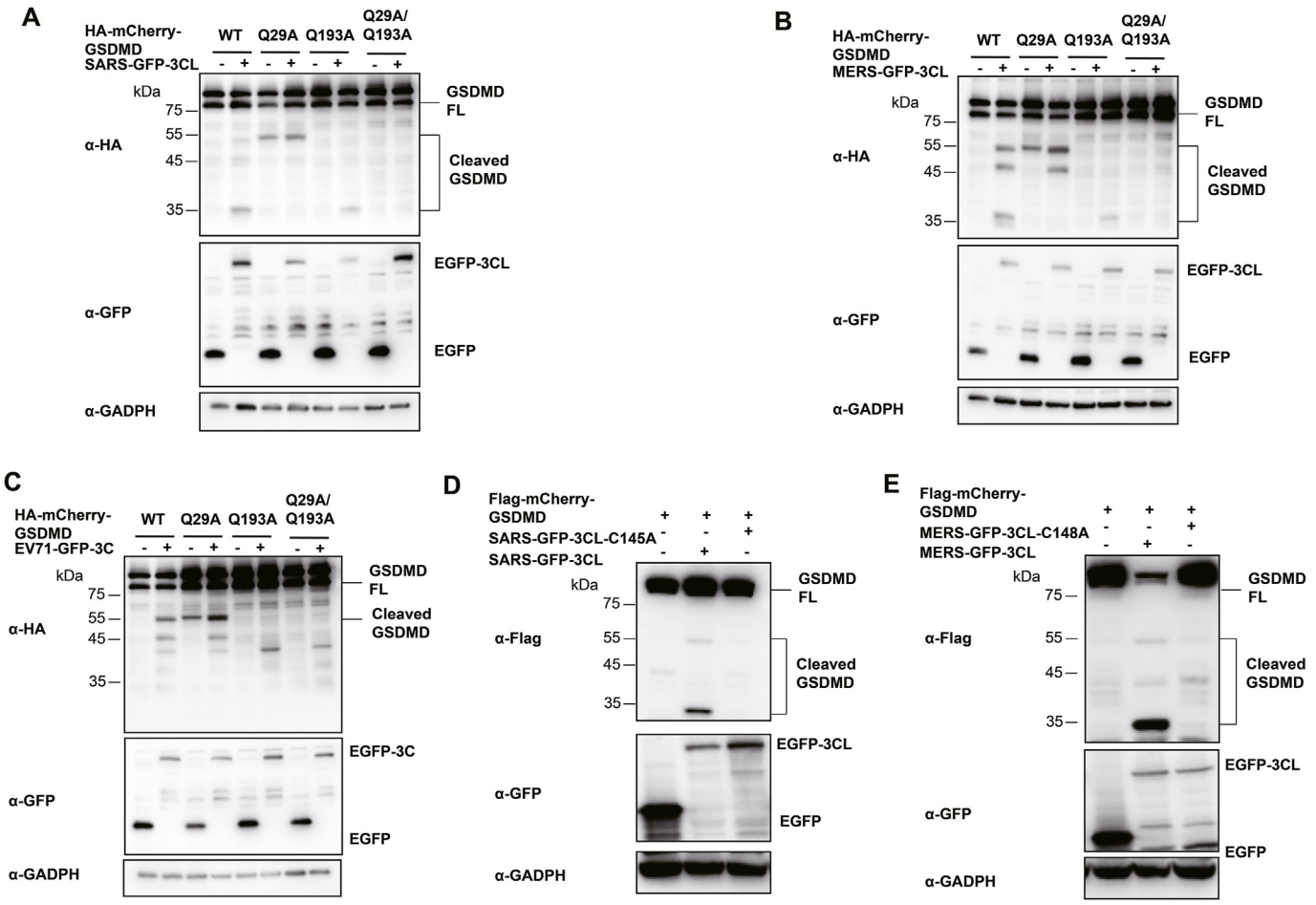

Fig. 5. Differences in the GSDMD cleavage sites of viral proteases from various viruses. **A–C** Western blot analysis of wild-type and mutant HA-mCherry-GSDMD cleavage by 3CL proteases from SARS-CoV (**A**), MERS-CoV (**B**), and 3C protease of EV71 (**C**) in 293T cells. **D–E** Western blot analysis of GSDMD cleavage by the wild-type and C145A mutant 3CL proteases from SARS-CoV (**D**) and the wild-type and C148A mutant 3CL proteases from MERS-CoV (**E**).

MERS-3CL-C148A, respectively. When the wild-type SARS or MERS 3CL protease was co-transfected with GSDMD, the GSDMD protein was observed to be cleaved into two distinct bands of approximately 55 kDa and 35 kDa (Fig. 5D and E). However, when co-transfected with the inactive mutants SARS-3CL-C145A or MERS-3CL-C148A and GSDMD, GSDMD cleavage was absent (Fig. 5D and E). These findings indicate that the cleavage of GSDMD protein by the 3CL proteases of SARS-CoV and MERS-CoV is reliant on their proteolytic activity.

DISCUSSION

Pyroptosis, an inflammatory form of programmed cell death, plays a dual role in viral infections. It can promote the clearance of infected cells and limit viral replication, but excessive pyroptosis may lead to tissue damage and contribute to disease pathogenesis. SARS-CoV-2 can directly activate GSDMD, triggering NET production and organ damage (Silva et al., 2022). Understanding the regulation of pyroptosis during viral infections is crucial for elucidating pathogenic mechanisms.

Viral proteases are essential for virus replication, immune evasion, and regulation of cell death pathways. The SARS-CoV-2 3CL protease primarily cleaves viral polyproteins into functional proteins essential for virus replication (Wang et al., 2022). Viruses hijack several immune regulatory proteins to inhibit the host antiviral immune response by suppressing the type I interferon response (Hui et al., 2021) and inhibiting apoptosis (Pan et al., 2023). Recently, many reports have shown that the SARS-CoV-2 3CL protease targets host proteins to modulate immune responses, such as the inhibition of IFN production (Zhang W. et al., 2021), the regulation of antiviral genes (Pablos et al., 2021; Zhang S. et al., 2021; Wu et al., 2023) and the activation of the NLRP1 or CARD8 inflammasome (Planès et al., 2022; Tsu et al., 2023). Our study identified GSDMD as a novel target of the SARS-CoV-2 3CL protease. We demonstrated that SARS-CoV-2 cleaves GSDMD at Q29 and Q193 via the 3CL protease, producing $GSDMD_{1–29}$ and $GSDMD_{1–193}$. These fragments disrupt $GSDMD_{1–275}$-induced pyroptosis and promote viral replication, suggesting a potential mechanism for SARS-CoV-2 pathogenesis.

The identification of GSDMD as a novel target of 3CL proteases is supported by several lines of evidence: (1) SARS-CoV-2 infection induces GSDMD cleavage in infected cells; (2) the expression of the SARS-CoV-2 3CL protease leads to GSDMD cleavage in mammalian cells; and (3) 3CL protease inhibitors block GSDMD cleavage and the catalytically inactive mutant of 3CL protease fails to cleave GSDMD. Our findings are consistent with recent studies showing that 3CL proteases from PEDV, Human coronavirus 229E (HCoV 229E) and SARS-CoV-2 cleave GSDMD to inhibit pyroptosis and facilitate viral replication (Planès et al., 2022; Shi et al., 2022; Martiáñez-Vendrell et al., 2024).

We also identified Q29 and Q193 as GSDMD cleavage sites for the SARS-CoV-2 3CL protease, consistent with the conserved QG/QS motifs predicted by Netconora. While a recent study reported similar results (Shen et al., 2024), two other groups identified only Q193 as a single cleavage site (Planès et al., 2022; Shi et al., 2022). This discrepancy may be due to the proximity of Q29 to the N-terminus, making its cleavage products difficult to detect. However, proteomic methods have confirmed that both Q29 and Q193 are 3CL protease recognition sites in GSDMD (Koudelka et al., 2021). Most recent study also confirmed that the SARS-CoV-2 3CL protease cleaves GSDMD at Q29, Q193 and H270, modulating pore formation to affect antiviral pyroptosis, viral

replication, and unconventional secretion, while extracellular 3CL protease retains activity to dampen platelet activation and inactivate antiviral interferon-λ1 (Grin et al., 2024). Collectively, these results suggest that the SARS-CoV-2 3CL protease cleaves $GSDMD_{1–275}$ to produce $GSDMD_{1–29}$ and $GSDMD_{1–193}$. Importantly, these GSDMD fragments cleaved by the SARS-CoV-2 3CL protease do not induce pyroptosis or inhibit viral replication. This finding is consistent with previous studies showing that viral proteases, such as the 3C protease of EV71 and the S273R protease of African swine fever virus, can cleave GSDMD to disrupt pyroptosis and promote viral replication (Lei et al., 2017; Zhao et al., 2022). Although GSDMD is well known to play a role in pyroptosis, it also regulates cellular homeostasis through its nonpyroptotic functions. For example, during the late stage of RANKL-induced osteoclastogenesis, GSDMD is cleaved by RIPK1 and caspase-8/-3 to generate the nonlytic p20 fragment (Li et al., 2022). Therefore, further research should investigate the nonpyroptotic roles of cleaved GSDMD fragments in SARS-CoV-2 replication and pathogenesis.

Notably, we also found that 3CL proteases from SARS-CoV and MERS-CoV cleave GSDMD at both Q29 and Q193, while the EV71 3C protease cleaves GSDMD only at Q193, which is consistent with a previous report (Shen et al., 2024), suggesting that GSDMD cleavage may be a common mechanism employed by different viruses to inhibit pyroptosis, although the preferred cleavage sites may vary among different viral proteases. Despite the 3CL protease of coronavirus and picornaviruses displaying some structural similarities, there are subtle structural differences in the substrate binding pockets, which could make these two proteases selective for substrates and inhibitors (Ramajayam et al., 2011). We hypothesize that structural differences between the two proteases, particularly in their substrate binding pockets, may contribute to their distinct cleavage specificities. Additionally, we explored potential amino acid sequence variations around the Q29 and Q193 sites in GSDMD that could influence protease recognition and cleavage efficiency. The different preferences between the 3CL protease from SARS-CoV-2 and 3C protease from EV71 and their substrate GSDMD need to be further studied based on structure biology.

CONCLUSIONS

In summary, our study confirmed the cleavage of GSDMD by the 3CL protease during SARS-CoV-2 infection. The double mutation of Q29 and Q193 completely abolishes GSDMD cleavage, indicating that the SARS-CoV-2 3CL protease cleave GSDMD at Q29 and Q193 to produce $GSDMD_{1-29}$ and $GSDMD_{1-193}$. Notably, these cleaved fragments do not induce pyroptosis or reduce viral replication, likely due to GSDMD inactivation. In conclusion, our findings reveal a mechanism by which SARS-CoV-2 hijacks the pyroptosis pathway to enhance its replication, suggesting potential therapeutic targets.

MATERIALS AND METHODS

Cell lines and culture

H1299-ACE2 cells were cultured in Gibco RP Basic MI 1640 medium (C11875500BT; Gibco). The human liver hepatocellular cancer cell line Huh7 (YB–H3110; ATCC), embryonic kidney cell line HEK293T (HEMCL-032; ATCC) and African green monkey kidney cell line Vero-E6 (CRL-1586; ATCC) were maintained in Dulbecco's modified Eagle's medium (DMEM, 12,100–046; Gibco). The media were supplemented with 10% fetal bovine serum (FBS, 10,099–141; Gibco) and 100 U/mL penicillin-streptomycin (15,140–122; Gibco). The cells were incubated at 37 °C with 5% CO_2.

Virus strains and infection

SARS-CoV-2 (accession number: MN996528.1) was propagated on Vero-E6 cells in DMEM supplemented with 2% FBS at 37 °C with 5% CO_2. SARS-CoV-2 virus infections were performed as described previously (Zhang X. et al., 2021). Briefly, cells were inoculated with SARS-CoV-2 at different multiplicities of infection (MOI = 0.01, 0.1 or 1) for 1 h at 37 °C. After removing the inoculum, the cells were cultured in DMEM supplemented with 2% FBS at 37 °C for 24 h before sample collection for Western blotting.

Plasmids and reagents

Plasmids expressing the GFP-tagged SARS-CoV-2 3CL protease (GFP-3CL) were constructed using the pEGFP-C1 vector. 3CL proteases from SARS-CoV (accession number: AY394980.1) and MERS-CoV, (accession number: NC_019843.3), as well as the 3C protease of EV71 (accession number: JN230523.1), were synthesized by Sangon Biotech and subsequently inserted into the pEGFP-C1 vector. Additionally, a catalytically inactive mutant of SARS-CoV-2 3CL protease (GFP-3CL-C145A), SARS-CoV (SARS-3CL-C145A) and MERS-CoV (MERS-3CL-C148A) proteases were also constructed by site-directed mutagenesis.

The GSDMD construct was generated in the pCMV-HA-N vector, with mCherry inserted between the HA tag or Flag tag and GSDMD (HA-mCherry-GSDMD or Flag-mCherry-GSDMD). Point mutations (Q29A, Q193A, and Q29A/Q193A) were introduced by site-directed mutagenesis. The Flag tagged GSDMB and GSDME construct were generated in the pCMV-Flag-N vector.

The GSDMD deletion mutants (aa 1–275, 276–484, 1–193, 194–484, 1–29, 30–484, 30–275, and 30–193) were constructed based on the full-length 3× Flag-tagged GSDMD plasmid. All the constructs mentioned above were validated by DNA sequencing.

The SARS-CoV-2 3CL protease inhibitor PF-00835231 (HY-137048) was purchased from MedChemExpress (Boras et al., 2021).

Cell viability and lactate dehydrogenase release assay

HEK293T cells were transfected with the indicated plasmids using Lipofectamine 2000 (Thermo Fisher Scientific). After 24 h, cell viability was assessed using the Cell Counting Kit-8 (CCK-8) assay (C0038; Beyotime), and cell death was measured by lactate dehydrogenase (LDH) release using an LDH Release Assay Kit (C0016; Beyotime) according to the manufacturer's instructions.

Real-time reverse transcription-PCR

After 24 h of transfection with the indicated plasmids, H1299-ACE2 cells were mock infected or infected with SARS-CoV-2 at an MOI of 0.01. At 24 h post infection, total RNA was extracted from the cells and supernatants by using TRIzol reagent (Invitrogen) according to the manufacturer's instructions. Reverse transcription and real-time PCR were performed using a HiScript III U + One Step qRT-PCR Probe Kit (Q225; Vazyme). The results were reported as the fold change using the ΔΔCT (where CT is the threshold cycle) method.

Western blot analysis

The cells were collected by centrifugation at 3000 rpm for 5 min at 4 °C and lysed in radioimmunoprecipitation assay (RIPA) buffer (P0013B; Beyotime) for 30 min. The lysates were subsequently centrifuged at 12,000 rpm for 10 min at 4 °C. Proteins were separated by SDS-PAGE and transferred to nitrocellulose membranes. The membranes were blocked with 5% non-fat dry milk, probed with the indicated primary antibodies overnight at 4 °C, and incubated with the corresponding IgG secondary antibodies for 1 h. Luminescent signals were detected using a Luminescent Image Analyser (SageCreation).

Antibodies against Flag (D6W5B) and HA (C29F4) were purchased from Cell Signaling Technology. Antibodies against the nucleoprotein (N) protein of SARS-CoV-2 (80027-1-RR), GFP (50430-2-AP) and GADPH

(60004-1-Ig) were purchased from Proteintech. A rabbit monoclonal antibody against GSDMD (ab209845) was purchased from Abcam.

$TCID_{50}$ assay

SARS-CoV-2 was titrated on Vero-E6 cells by a $TCID_{50}$ assay. Briefly, Vero-E6 cells were seeded into 96-well plates and then infected with 100 μL of a serial 10-fold dilution of viral stock. After 4 days, the cytopathic effect (CPE) was observed, and 50% tissue culture infective doses ($TCID_{50}$) were calculated using the Reed and Muench method.

Statistics

Two-tailed Student's *t*-test was used for two-group comparisons. *P* values < 0.05, < 0.01, and < 0.001 were considered significant (*, **, and ***, respectively).

DATA AVAILABILITY

The complete sequence of SARS-CoV-2 used in this work has been deposited with National Center for Biotechnology Information under accession number MN996528.1. Original data and materials will be available upon requests.

ETHICS STATEMENT

This article does not contain any studies with human or animal subjects performed by any of the authors.

AUTHOR CONTRIBUTIONS

Yecheng Zhang: conceptualization, data curation, formal analysis, investigation, methodology, writing-original draft. Xinlei Ji: data curation, investigation. Dan Huang: formal analysis. Gen Lu: funding acquisition, supervision, writing-review&editing. Xinwen Chen: conceptualization, funding acquisition, project administration, supervision, writing-review&editing.

CONFLICT OF INTEREST

The authors declare that they have no conflicts of interest. Prof. Xinwen Chen is an editorial board member for *Virologica Sinica* and was not involved in the editorial review or the decision to publish this article.

ACKNOWLEDGEMENTS

This work was supported by the National Natural Science Foundation of China (82370015). Experiments related to SARS-CoV-2 were carried out at the National Biosafety Laboratory. We are particularly grateful to Tao Du, Jin Xiong and Min Hou from the National Biosafety Laboratory and the team running the laboratory for their work. We extend our special thanks to Prof. Rongjuan Pei and Hao Sun, Yi Zheng, Yongli Zhang from Chinese Academy of Sciences for their significant assistance in this study. We also thank the other members of the Xinwen Chen and Gen Lu's lab for their constructive comments.

REFERENCES

Anand, K., Ziebuhr, J., Wadhwani, P., Mesters, J.R., Hilgenfeld, R., 2003. Coronavirus main proteinase (3CLpro) structure: basis for design of anti-SARS drugs. Science 300, 1763–1767.

Boras, B., Jones, R.M., Anson, B.J., Arenson, D., Aschenbrenner, L., Bakowski, M.A., Beutler, N., Binder, J., Chen, E., Eng, H., et al., 2021. Preclinical characterization of an intravenous coronavirus 3CL protease inhibitor for the potential treatment of COVID19. Nat. Commun. 12, 6055.

Broz, P., Dixit, V.M., 2016. Inflammasomes: mechanism of assembly, regulation and signalling. Nat. Rev. Immunol. 16, 407–420.

Fung, M., Otani, I., Pham, M., Babik, J., 2021. Zoonotic coronavirus epidemics: severe acute respiratory syndrome, Middle East respiratory syndrome, and coronavirus disease 2019. Ann. Allergy Asthma Immunol. 126, 321–337.

Grin, P.M., Baid, K., De Jesus, H.C.R., Kozarac, N., Bell, P.A., Jiang, S.Z., Kappelhoff, R., Butler, G.S., Leborgne, N.G.F., Pan, C., et al., 2024. SARS-CoV-2 3CL(pro) (main protease) regulates caspase activation of gasdermin-D/E pores leading to secretion and extracellular activity of 3CL(pro). Cell Rep. 43, 115080.

Hui, X., Zhang, L., Cao, L., Huang, K., Zhao, Y., Zhang, Y., Chen, X., Lin, X., Chen, M., Jin, M., 2021. SARS-CoV-2 promote autophagy to suppress type I interferon response. Signal Transduct. Targeted Ther. 6, 180.

Jin, Z., Du, X., Xu, Y., Deng, Y., Liu, M., Zhao, Y., Zhang, B., Li, X., Zhang, L., Peng, C., et al., 2020. Structure of M(pro) from SARS-CoV-2 and discovery of its inhibitors. Nature 582, 289–293.

Jorgensen, I., Miao, E.A., 2015. Pyroptotic cell death defends against intracellular pathogens. Immunol. Rev. 265, 130–142.

Koudelka, T., Boger, J., Henkel, A., Schönherr, R., Krantz, S., Fuchs, S., Rodríguez, E., Redecke, L., Tholey, A., 2021. N-terminomics for the identification of in vitro substrates and cleavage site specificity of the SARS-CoV-2 main protease. Proteomics 21, e2000246.

Lei, X., Zhang, Z., Xiao, X., Qi, J., He, B., Wang, J., 2017. Enterovirus 71 inhibits pyroptosis through cleavage of gasdermin D. J. Virol. 91, e01069-17.

Li, M., Yang, D., Yan, H., Tang, Z., Jiang, D., Zhang, J., Chi, Z., Nie, W., Zhen, W., Yu, W., et al., 2022. Gasdermin D maintains bone mass by rewiring the endo-lysosomal pathway of osteoclastic bone resorption. Dev. Cell 57, 2365–2380.e2368.

Liu, X., Zhang, Z., Ruan, J., Pan, Y., Magupalli, V.G., Wu, H., Lieberman, J., 2016. Inflammasome-activated gasdermin D causes pyroptosis by forming membrane pores. Nature 535, 153–158.

Ma, J., Zhu, F., Zhao, M., Shao, F., Yu, D., Ma, J., Zhang, X., Li, W., Qian, Y., Zhang, Y., et al., 2021. SARS-CoV-2 nucleocapsid suppresses host pyroptosis by blocking Gasdermin D cleavage. EMBO J. 40, e108249.

Martiáñez-Vendrell, X., Bloeme-Ter Horst, J., Hutchinson, R., Guy, C., Bowie, A.G., Kikkert, M., 2024. Human coronavirus 229E infection inactivates pyroptosis executioner gasdermin D but ultimately leads to lytic cell death partly mediated by gasdermin E. Viruses 16, 898.

Moustaqil, M., Ollivier, E., Chiu, H.P., Van Tol, S., Rudolffi-Soto, P., Stevens, C., Bhumkar, A., Hunter, D.J.B., Freiberg, A.N., Jacques, D., et al., 2021. SARS-CoV-2 proteases PLpro and 3CLpro cleave IRF3 and critical modulators of inflammatory pathways (NLRP12 and TAB1): implications for disease presentation across species. Emerg. Microb. Infect. 10, 178–195.

Pablos, I., Machado, Y., De Jesus, H.C.R., Mohamud, Y., Kappelhoff, R., Lindskog, C., Vlok, M., Bell, P.A., Butler, G.S., Grin, P.M., et al., 2021. Mechanistic insights into COVID-19 by global analysis of the SARS-CoV-2 3CL(pro) substrate degradome. Cell Rep. 37, 109892.

Pan, P., Ge, W., Lei, Z., Luo, W., Liu, Y., Guan, Z., Chen, L., Yu, Z., Shen, M., Hu, D., et al., 2023. SARS-CoV-2 N protein enhances the anti-apoptotic activity of MCL-1 to promote viral replication. Signal Transduct. Targeted Ther. 8, 194.

Planès, R., Pinilla, M., Santoni, K., Hessel, A., Passemar, C., Lay, K., Paillette, P., Valadão, A.C., Robinson, K.S., Bastard, P., et al., 2022. Human NLRP1 is a sensor of pathogenic coronavirus 3CL proteases in lung epithelial cells. Mol. Cell 82, 2385–2400.e2389.

Ramajayam, R., Tan, K.P., Liang, P.H., 2011. Recent development of 3C and 3CL protease inhibitors for anti-coronavirus and anti-picornavirus drug discovery. Biochem. Soc. Trans. 39, 1371–1375.

Sborgi, L., Rühl, S., Mulvihill, E., Pipercevic, J., Heilig, R., Stahlberg, H., Farady, C.J., Müller, D.J., Broz, P., Hiller, S., 2016. GSDMD membrane pore formation constitutes the mechanism of pyroptotic cell death. EMBO J. 35, 1766–1778.

Shen, S., Guo, H., Li, Y., Zhang, L., Tang, Y., Li, H., Li, X., Wang, P.H., Yu, X.F., Wei, W., 2024. SARS-CoV-2 and oncolytic EV-D68-encoded proteases differentially regulate pyroptosis. J. Virol. 98, e0190923.

Shi, F., Lv, Q., Wang, T., Xu, J., Xu, W., Shi, Y., Fu, X., Yang, T., Yang, Y., Zhuang, L., et al., 2022. Coronaviruses Nsp5 antagonizes porcine gasdermin D-mediated pyroptosis by cleaving pore-forming p30 fragment. mBio 13, e0273921.

Shi, J., Zhao, Y., Wang, K., Shi, X., Wang, Y., Huang, H., Zhuang, Y., Cai, T., Wang, F., Shao, F., 2015. Cleavage of GSDMD by inflammatory caspases determines pyroptotic cell death. Nature 526, 660–665.

Silva, C.M.S., Wanderley, C.W.S., Veras, F.P., Gonçalves, A.V., Lima, M.H.F., Toller-Kawahisa, J.E., Gomes, G.F., Nascimento, D.C., Monteiro, V.V.S., Paiva, I.M., et al., 2022. Gasdermin-D activation by SARS-CoV-2 triggers NET and mediate COVID-19 immunopathology. Crit. Care 26, 206.

Tsu, B.V., Agarwal, R., Gokhale, N.S., Kulsuptrakul, J., Ryan, A.P., Fay, E.J., Castro, L.K., Beierschmitt, C., Yap, C., Turcotte, E.A., et al., 2023. Host-specific sensing of coronaviruses and picornaviruses by the CARD8 inflammasome. PLoS Biol. 21, e3002144.

Tsu, B.V., Fay, E.J., Nguyen, K.T., Corley, M.R., Hosuru, B., Dominguez, V.A., Daugherty, M.D., 2021. Running with scissors: evolutionary conflicts between viral proteases and the host immune system. Front. Immunol. 12, 769543.

Wang, H., Pei, R., Li, X., Deng, W., Xing, S., Zhang, Y., Zhang, C., He, S., Sun, H., Xiao, S., et al., 2022. The structure-based design of peptidomimetic inhibitors against SARS-CoV-2 3C like protease as Potent anti-viral drug candidate. Eur. J. Med. Chem. 238, 114458.

Wu, Y., Li, M., Tian, J., Yan, H., Pan, Y., Shi, H., Shi, D., Chen, J., Guo, L., Feng, L., 2023. Broad antagonism of coronaviruses nsp5 to evade the host antiviral responses by cleaving POLDIP3. PLoS Pathog. 19, e1011702.

Yang, H., Rao, Z., 2021. Structural biology of SARS-CoV-2 and implications for therapeutic development. Nat. Rev. Microbiol. 19, 685–700.

Yang, H., Xie, W., Xue, X., Yang, K., Ma, J., Liang, W., Zhao, Q., Zhou, Z., Pei, D., Ziebuhr, J., et al., 2005. Design of wide-spectrum inhibitors targeting coronavirus main proteases. PLoS Biol. 3, e324.

Yao, Y., Sun, H., Chen, Y., Tian, L., Huang, D., Liu, C., Zhou, Y., Wang, Y., Wen, Z., Yang, B., et al., 2023. RBM24 inhibits the translation of SARS-CoV-2 polyproteins by targeting the 5'-untranslated region. Antivir. Res. 209, 105478.
Yogarajah, T., Ong, K.C., Perera, D., Wong, K.T., 2017. AIM2 inflammasome-mediated pyroptosis in enterovirus A71-infected neuronal cells restricts viral replication. Sci. Rep. 7, 5845.
Zhang, L., Lin, D., Sun, X., Curth, U., Drosten, C., Sauerhering, L., Becker, S., Rox, K., Hilgenfeld, R., 2020. Crystal structure of SARS-CoV-2 main protease provides a basis for design of improved α-ketoamide inhibitors. Science 368, 409–412.
Zhang, S., Wang, J., Cheng, G., 2021. Protease cleavage of RNF20 facilitates coronavirus replication via stabilization of SREBP1. Proc. Natl. Acad. Sci. U. S. A. 118, e2107108118.
Zhang, W., Ma, Z., Wu, Y., Shi, X., Zhang, Y., Zhang, M., Zhang, M., Wang, L., Liu, W., 2021. SARS-CoV-2 3C-like protease antagonizes interferon-beta production by facilitating the degradation of IRF3. Cytokine 148, 155697.
Zhang, X., Hao, H., Ma, L., Zhang, Y., Hu, X., Chen, Z., Liu, D., Yuan, J., Hu, Z., Guan, W., 2021. Methyltransferase-like 3 modulates severe acute respiratory syndrome coronavirus-2 RNA N6-methyladenosine modification and replication. mBio 12, e0106721.
Zhao, G., Li, T., Liu, X., Zhang, T., Zhang, Z., Kang, L., Song, J., Zhou, S., Chen, X., Wang, X., et al., 2022. African swine fever virus cysteine protease pS273R inhibits pyroptosis by noncanonically cleaving gasdermin D. J. Biol. Chem. 298, 101480.
Zheng, Z., Deng, W., Lou, X., Bai, Y., Wang, J., Zeng, H., Gong, S., Liu, X., 2020. Gasdermins: pore-forming activities and beyond. Acta Biochim. Biophys. Sin. 52, 467–474.
Zhou, P., Yang, X.L., Wang, X.G., Hu, B., Zhang, L., Zhang, W., Si, H.R., Zhu, Y., Li, B., Huang, C.L., et al., 2020. A pneumonia outbreak associated with a new coronavirus of probable bat origin. Nature 579, 270–273.
Zhu, S., Ding, S., Wang, P., Wei, Z., Pan, W., Palm, N.W., Yang, Y., Yu, H., Li, H.B., Wang, G., et al., 2017. Nlrp9b inflammasome restricts rotavirus infection in intestinal epithelial cells. Nature 546, 667–670.